B

J Mater Sci (2018) 53:10543–10553

Polymers

Effect of temperature, crystallinity and molecular chain orientation on the thermal conductivity of polymers: a case study of PLLA

F

Lu Bai[1], Xing Zhao[1], Rui-Ying Bao[1], Zheng-Ying Liu[1], Ming-Bo Yang[1], and Wei Yang[1,*]

D

[1] *State Key Laboratory of Polymer Materials Engineering, College of Polymer Science and Engineering, Sichuan University, Chengdu 610065, Sichuan, China*

E

Received: 8 January 2018
Accepted: 6 April 2018
Published online: 19 April 2018

ABSTRACT

The crystallinity of semicrystalline polymers and molecular orientation of polymer have long been considered to be significant influencing factors on the thermal conductivity of polymer materials, but more clear-cut understanding on their impact on the thermal conductivity is still needed. In this work, poly-L-lactide (PLLA), whose crystallinity and orientation can be adjusted in a wide range, is selected to discuss the effect of degree of crystallinity and orientation on the thermal conductivity of PLLA. Meanwhile, the influence of temperature on the thermal conductivity is also discussed. PLLA compression-molded samples were heat-treated at 120 °C to tune the crystallinity of the samples, while the degrees of orientation were tuned by stretching the amorphous PLLA bars at 60 °C to different strains. It is found that environmental temperature of application affects the thermal conductivity obviously and the glass transition temperature of polymers shows a strong influence on the thermal conductivity of PLLA. Below T_g, the thermal conductivity of PLLA with different crystallinity increases with temperature and when the temperature is higher than T_g, the thermal conductivity of PLLA with different crystallinity decreases remarkably. It is also demonstrated that the thermal conductivity of PLLA increases with the increase in crystallinity, and the tensile strain linearly increases the thermal conductivity in the direction of molecular orientation and decreases the thermal conductivity in the perpendicular direction, which are in agreement with other semicrystalline polymers that has been reported.

Address correspondence to E-mail: weiyang@scu.edu.cn

https://doi.org/10.1007/s10853-018-2306-4

C

Introduction

With the rapid development of science and technologies, electric products are more and more highly integrated, which urgently pushes the exploitation of effective thermal management materials including thermally conductive polymers and polymer composites to be applied in various applications [1–7], such as packaging, electronic devices and energy storage. However, bulk polymers generally exhibit very low thermal conductivity (TC) in the range of 0.1–0.5 W/(mK) [8, 9], so the development of polymer materials with enhanced thermal conductivity has become a great challenge to meet great increasing demands [10–15]. It has been accepted that the polymer matrix plays a crucial role in the overall TC of polymer composites [16]. It is therefore necessary to clearly clarify the influence of important factors such as crystallinity and molecular orientation on the TC of polymers.

Generally, crystalline polymers exhibit higher TC than amorphous polymers due to the ordered structure, while the random chain conformation in amorphous polymers reduces the phonon mean free path and causes phonon scattering [17]. In early study, Hansen et al. [18] reported that the TC of high density polyethylene can be improved by increasing the crystallinity and lamellar thickness via tuning processing conditions. Subsequently, Choy and coworker [19] found that the influence of crystallinity on the TC of polyethylene terephthalate (PET) was affected by temperature. The TC of PET decreases with increasing crystallinity at low temperature, but increases with crystallinity at temperatures above 30 K. The peculiar behavior was interpreted from the increasing thermal boundary resistance due to acoustic mismatch at amorphous–crystalline interface when the temperature is lowered. Crystallization was also reported to be responsible for the higher TC in other semicrystalline polymers [20, 21]. The higher the crystallinity, the higher the thermal conductivity.

As heat transports more easily along polymer chains than perpendicular to the polymer chain, polymers exhibit significant anisotropy in their thermally conductive properties [22]. Numerous experimental studies on polymer chain orientation for TC enhancement have been reported. As a typical semicrystalline polymer, polyethylene (PE) has been mostly used to study the effect of orientation on TC [18, 23–28]. TC of other semicrystalline polymers stretched to different draw ratio including polyoxymethylene (POM), polypropylene (PP), polyvinylidene fluoride (PVDF) and PET was also studied [29]. The general result is that TC parallel to the orientation direction rapidly increases with increasing strain or draw ratio, while TC perpendicular to the orientation direction decreases slightly. But in these studies on the effect of the orientation, TC was also influenced by the crystallization nature of the polymers. To clarify how chain alignment affects TC during drawing, purely amorphous polymers were studied [30–34]. Early studies [31, 32] showed that the TC of stretched polymethyl methacrylate (PMMA) and polystyrene (PS) can be increased in the stretching direction, but the increase was small. However, it was found recently that polythiophene nanofibers can achieve a TC up to 4.4 W/(m K), more than 20 times greater than the bulk polymer through chain alignment [34]. Lu et al. [35] also evidenced the molecular alignment in amorphous region played a very important role in the enhancement of thermal conductivity of semicrystalline polyethylene oxide (PEO) fiber.

PLLA is a plant-derived biodegradable polymer material. However, low thermal conductivity restricts its application in engineering and electronic fields. To expand the applications of PLLA, many studies have been conducted to improve the TC of PLLA via compounding with thermally conductive fillers [36–41], but the basic influencing factors from the polymer itself have not been well addressed, which is hopefully to provide supporting for fabrication of high thermally conductive PLLA composites. Also, owing to that PLLA exhibits very low crystallization kinetics [42–44], the amorphous state by quenching and a wide range of degrees of crystallinity by isothermal crystallization at different temperature for different periods of time can be easily achieved [45]. These features provide a good candidate to elucidate the effect of crystallinity and molecular orientation on the TC of semicrystalline polymers.

In this study, the crystallinity of PLLA was tuned by melt crystallization at 120 °C for different minutes. Various degrees of orientation of PLLA were realized by stretching the amorphous PLLA bars at 60 °C with the same speed to different strains. WAXD was carried out to characterize the crystallinity and degree of orientation of PLLA. DSC, density measurement and laser flash method were performed together to reveal

the relation between TC and crystallinity, temperature and orientation of molecular chains. The results showed that TC of PLLA with different crystallinity was affected obviously by ambient temperature and the maximum value appeared at T_g. TC of PLLA increases with increasing crystallinity, and TC of PLLA parallel to the orientation direction increases with increasing tensile strain, while the one perpendicular to the stretching direction decreases with increasing strain. These results can further manifest the effect of crystallinity and orientation on the thermal conductivity of semicrystalline polymers. Also, this systematic study can provide supporting for fabricating enhanced thermally conductive PLLA composites.

Experimental section

Materials and sample preparation

PLLA (trade name 4032D, Nature Works LLC) was used. The average weight molecular weight (M_w) and the polydispersity index (PDI) are 2.1 × 10^5 g/mol and 1.7. The melting temperature is 167.2 °C, measured by differential scanning calorimetry at a heating rate of 10 °C/min.

PLLA granules were dried in a blast drying oven at 60 °C for 12 h, and then melted in the mixer of a torque rheometer with a rotational speed of 50 rpm at 190 °C for 5 min. After that, the resulted materials were compressed into sheets with the thickness of about 0.5 mm at 190 °C for 3 min under a pressure of 10 MPa. The melted PLLA sheet was immediately transferred to isothermal crystallization at 120 °C for different minutes (0, 5, 8, 10, 11, 12, 13 and 40 min) under a pressure of 10 MPa and then cooled quickly to obtain samples with different crystallinity. The resulted samples were designated as 120-*X* min, in which *X* stands for the compression time at 120 °C. Round disks with the diameter of 12.7 mm were cut from the 120-*X* min PLLA sheets for WAXD and thermal diffusivity tests. Rectangular-shaped sample bars with the dimension of 20 mm (width) × 80.0 mm (length) were cut from amorphous 120-0 min PLLA sheets, and then stretched uniaxially at 60 °C using an Instron 5967 universal material testing machine at a stretching rate of 20 mm/min. The tensile strain was controlled to be 0.5, 1, 2, 3 and 4. The stretched bars designated as 60-20-*Y*, in which *Y* stands for the tensile strain, were measured by 2D wide angel X-ray diffraction (WAXD) to determine the degree orientation. Both the through-plane and in-plane thermal diffusivities of the stretched bars were tested.

Characterization

WAXD measurements and data analysis

WAXD measurement of PLLA compression sheets isothermally crystallized at 120 °C for different minutes was performed on a Rigaku Ultima IV diffractometer with a Cu Kα radiation source (λ = 0.154 nm, 40 kV, 25 mA) in the scanning range of 2θ = 5°–60° at a scan speed of 10°/min at room temperature. The crystallinity was determined from the fractional area of the crystalline peaks to the total area [46].

WAXD measurement of PLLA samples stretched to different strains at 60 °C with the speed of 20 mm/min was carried out on a Bruker D8 DISCOVER 2D X-ray diffractometer with the reflection mode. The X-ray was generated using ImS micro Focus X-ray source generator with Cu target (λ = 0.154 nm, 40 kV, 40 mA). The 2D X-ray diffraction patterns were recorded on a VANTEC-500 detector system with a pixel size of 68 × 68 mm^2. The distance from the sample to detector was 198 mm. The spot size of the beam was 0.5 mm.

Density measurement

The density of PLLA compression-molded samples with different crystallinity was measured by using MH-120E density meter according to Archimedes principle.

Differential scanning calorimetry (DSC) measurement

The empty pan, sapphire standard and PLLA compression-molded samples with different crystallinity were measured by DSC (Q20, TA company). Samples were measured from − 80 to 90 °C with heating rate of 10 °C/min under nitrogen gas flow of 50 mL/min.

Thermal conductivity measurement by laser flash method

The sample preparation processes for the thermal diffusivity measurements are outlined in Fig. S1. Before testing, the thickness and length or diameter

of the samples were measured, and then both surfaces of the samples were evenly sprayed with a thin graphite layer. The sample was then fixed according to the required test pattern and placed in the test chamber (LFA 467, Netzsch). PLLA compression-molded samples with different crystallinity were tested in the temperature ranging from − 70 to 80 °C, while the PLLA stretched samples with different degree of orientation were tested at 25 °C.

Results and discussion

Effect of temperature and crystallinity on the thermal conductivity of PLLA

WAXD profiles of PLLA compression-molded samples isothermally crystallized at 120 °C for different period of time are shown in Fig. 1. It can be seen that the quenched PLLA compression-molded sample without isothermal crystallization (120-0 min) shows only a very broad diffraction peak of amorphous phase without any traces of crystalline peaks, clearly showing the amorphous nature of the sample owing to the extremely slow crystallization kinetics of PLLA. After isothermal crystallizing at 120 °C, the WAXD profile of the isothermally crystallized PLLA samples shows three peaks at 2θ = 16.7°, 19.0° and 22.3°, respectively, corresponding to the diffraction peaks of (200)/(110), (203) and (015) planes of α crystalline structure of PLLA. The diffraction intensity of the peaks increases with the extension of isothermal crystallization time, showing that isothermal treatment at 120 °C can effectively promote the crystallization of PLLA. By Gauss fitting of the WAXD profiles, the crystallinity of all the samples was calculated and is listed in Table 1. The results demonstrate that the crystallinity of PLLA isothermally crystallized at 120 °C increases with the extension of isothermal crystallizing time, and can even reach up to a level higher than 50%.

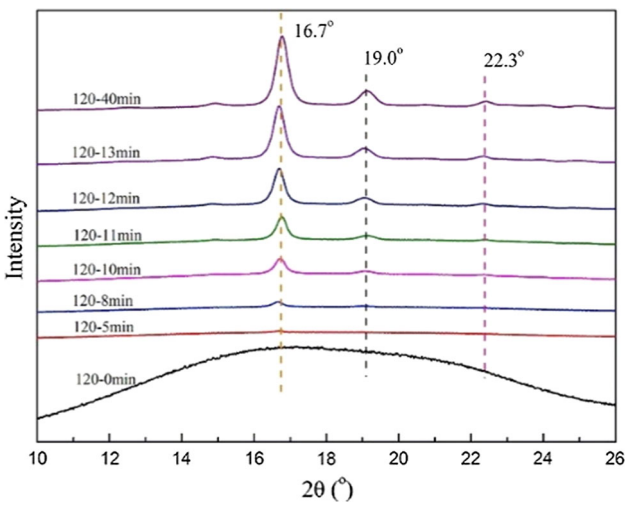

Figure 1 XRD profiles of PLLA compression-molded sheets isothermally crystallized at 120 °C for different time.

The different crystallinity of PLLA samples leads to the differences of densities, which are listed in Table 2. It can be seen that although the crystallinity varies in a great range after crystallizing at 120 °C for different time, the change in density, showing a slight increasing trends, is quite limited. However, when the crystallinity increases, the ratio of the ordered molecular chains in the system increases, leading to the decrease in the volume of the sample. That is why the density of PLLA increases a little with the increasing of crystallinity.

The specific heat (C_p) was obtained by DSC Q20 (TA Instruments, America) at a heating rate of 10 °C/min. The C_p values of PLLA compression samples with different crystallinity are calculated by Eq. (1):

$$C_p = C_{p'} m' h / (mH) \quad (1)$$

where C_p and $C_{p'}$, m and m', h and H are the specific heat, the weight and the heat flow of PLLA sample and sapphire standard, respectively. The specific heat of sapphire standard is given in the DSC software.

The calculated specific heat of PLLA samples is shown in Fig. 2. It shows that the specific heat increases linearly before 50 °C. An abrupt increase in the specific heat is observed in the glass transition temperature range (50–70 °C), resulting from the change of free volume of PLLA [47], and then specific heat remains constant for the samples with given crystallinity after T_g. Thermal diffusivities of PLLA samples with different crystallinity were measured by laser flash method, which is a non-contact transient thermal measurement method widely used for measuring the thermal diffusivity (α). With all these parameters, the thermal conductivity of the samples can be derived through Eq. (2):

$$k = \alpha \times \rho \times C_p \quad (2)$$

where ρ is the bulk density and C_p is the specific heat at a given pressure.

The thermal diffusivity and the thermal conductivity of PLLA samples with different crystallinity are

Table 1 Crystallinity of PLLA samples isothermally crystallized at 120 °C for different time

Sample code	120-0	120-5	120-8	120-10	120-11	120-12	120-13	120-40
X_c (%)	0	4	11	19	24	33	40	56

Table 2 Density of PLLA samples isothermally crystallized at 120 °C for different time

Sample code	120-0	120-5	120-8	120-10	120-11	120-12	120-13	120-40
Density (g/cm^3)	1.243	1.245	1.245	1.246	1.246	1.248	1.249	1.254

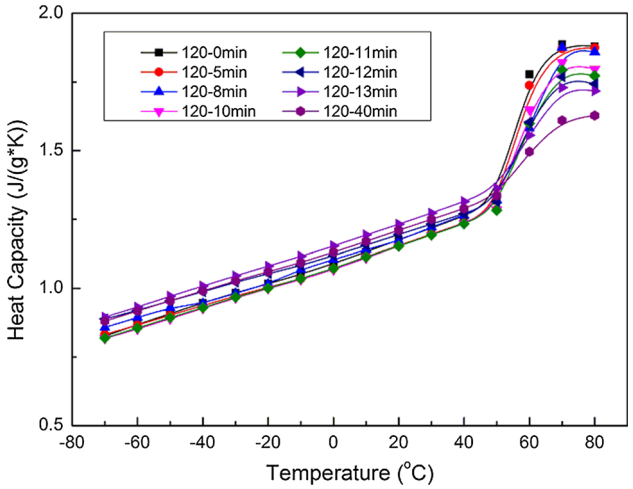

Figure 2 Specific heat of PLLA compression-molded sheets with different crystallinity between − 70 and 80 °C.

shown in Fig. 3. Figure 3a shows that the thermal diffusivity of PLLA samples with different crystallinity reduces moderately due to the decrease in the phonon mean free path when the temperature rises, but drops abruptly within the glass transition temperature range. Taking 120-40 as an example, the thermal diffusivity decreases by 0.033 mm^2/s from − 70 to 60 °C, but decreases by 0.017 mm^2/s sharply only from 60 to 80 °C. The sudden drop can be explained in terms of molecular mobility [48]. But it should be noted that the abrupt drop trend around T_g becomes gentler with increasing crystallinity of PLLA samples. It can be understood from the fact that the crystallized fractions refine the amorphous phase of PLLA to a certain degree and hinder the molecular motion in amorphous regions which will reduce the phonon mean free path, especially at temperatures near the glass transition.

Figure 3b shows the relationship between thermal conductivity of PLLA samples with different crystallinity and temperature. It can be found that the environmental temperature affects the thermal conductivity obviously. Notably, the glass transition temperature exerts a great influence on the thermal conductivity. In the glass state below T_g, thermal conductivities of all the PLLA samples with different crystallinity increase with temperature. In this temperature range, two mechanisms with opposite effects operate [48]. The thermal diffusivity decreases with temperature increasing, while the increase in

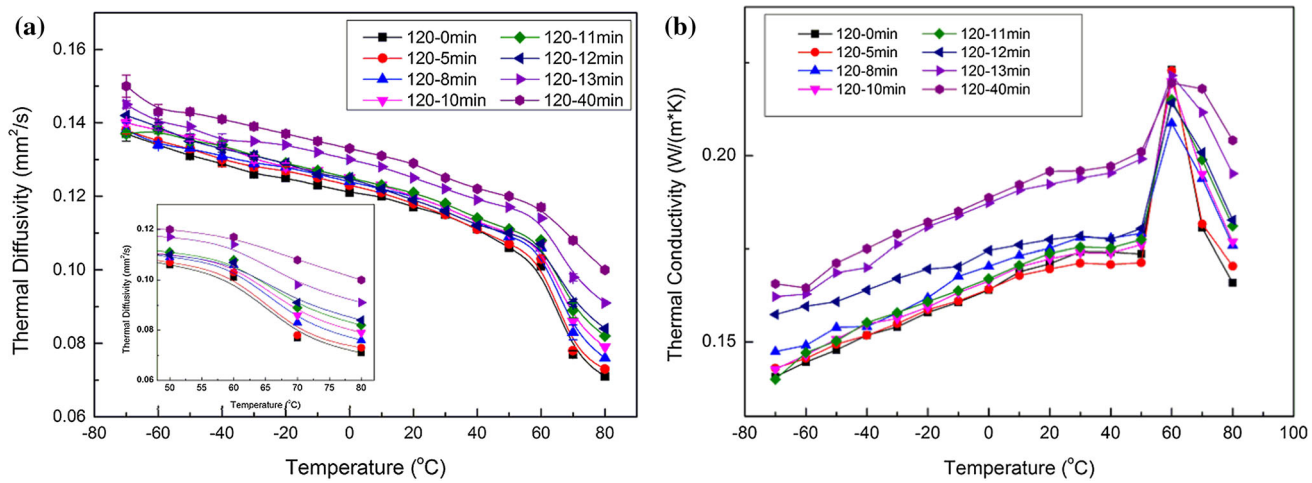

Figure 3 Thermal diffusivity (**a**) and conductivity (**b**) of PLLA samples with different crystallinity between − 70 and 80 °C.

specific heat attributes more to the thermal conductivity. The net effect is a smooth and moderate increase in thermal conductivity with temperature increasing. When the temperature is further increased, the amorphous phase of PLLA sample gets into rubbery state, and the molecular chains of the amorphous phase begin to move, leading to a great reduction in the phonon mean free path. So, the thermal conductivity decreases remarkably. Such a process produces the maximum of the thermal conductivity near the glass transition temperature in the range of the measured temperatures. Meanwhile, it also can be seen that the thermal conductivity of PLLA samples increases with the increase in crystallinity of PLLA.

To further analyze the effect of the crystallinity on the thermally conductive properties of PLLA, the thermal diffusivity, specific heat and thermal conductivity of PLLA samples at different temperatures are presented as a function of crystallinity in Fig. 4. The specific heat changes linearly with the increase in crystallinity of PLLA at different temperatures. The slope of the fitting curve decreases from 0.118 to − 0.46 with increasing temperature. It shows that the specific heat of PLLA decreases with increasing crystallinity when the temperature is higher than T_g, due to that Cp for amorphous phase is larger than crystal phase [49]. However, specific heat of PLLA samples increases slowly with the increasing crystallinity at temperatures below T_g. Thermal diffusivity of PLLA increases linearly with increasing crystallinity, and the increasing rate keeps stable at the temperatures below T_g, while the increasing rate increases after T_g. When the amorphous phase is in the rubber state, the motion of the molecular chains reduces the phonon mean free path obviously, while with the increasing crystallinity, the mean free path increases distinctly. That is why the thermal diffusivity increases obviously with increasing crystallinity. Therefore, the thermal conductivity of PLLA samples as a result of the specific heat and thermal diffusivity increases with increasing crystallinity.

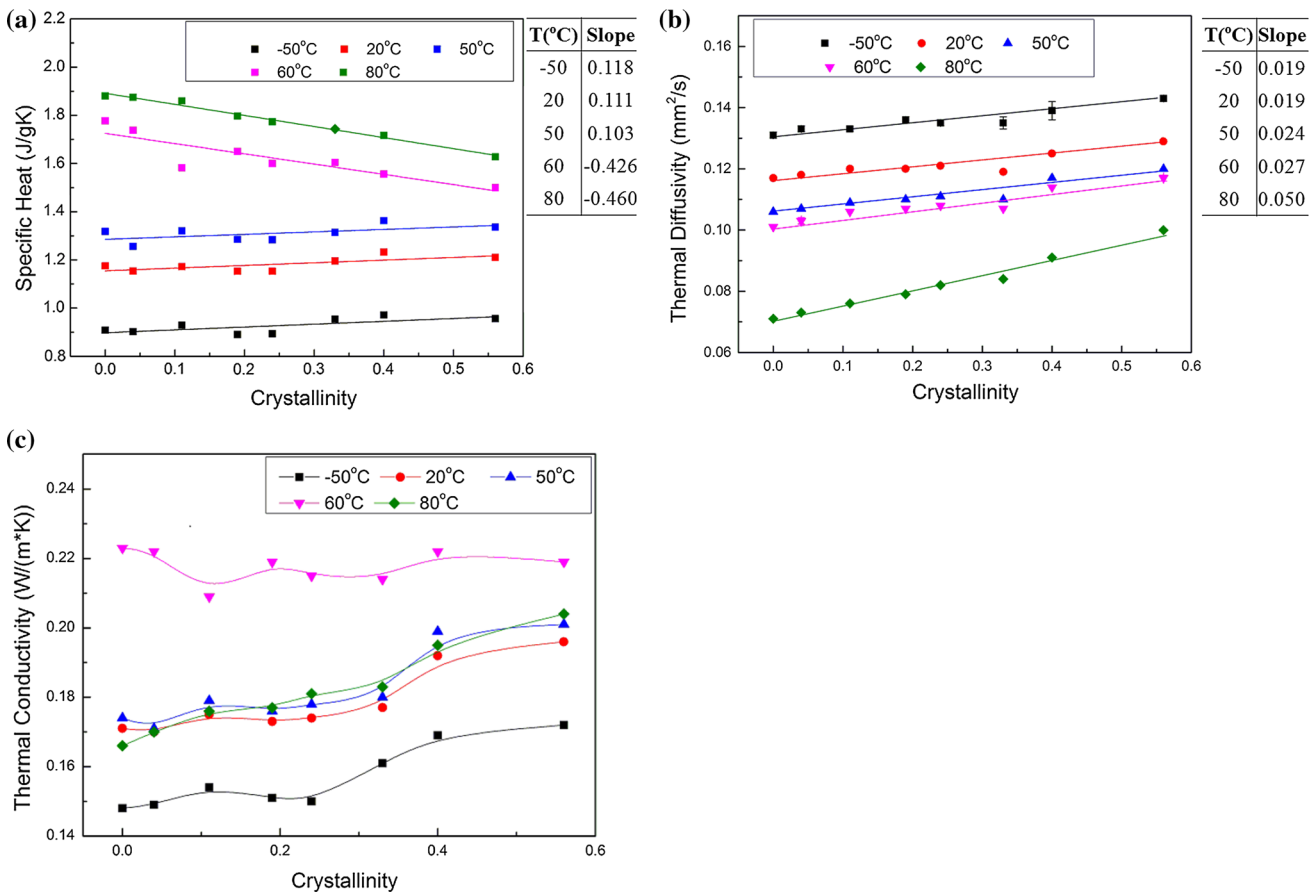

Figure 4 Variation of Cp (**a**), thermal diffusivity (**b**) and thermal conductivity (**c**) of PLLA samples with different degree of crystallinity at given temperatures.

Though the specific heat decreases with increasing crystallinity after T_g, the thermal diffusivity compensates more for the thermal conductivity. The increase in thermal conductivity of PLLA samples with increasing crystallinity is in agreement with that of other semi-crystallized polymers. However, it should be noted that TC of PLLA is not significantly increased with crystallinity. TC of PLLA with the crystallinity of 56% (120-40) is 0.196 W/mK at 20 °C, only 0.025 W/mK larger than the thermal conductivity of amorphous PLLA (120-0).

Effect of molecular orientation on the thermal conductivity of PLLA

To obtain PLLA with different degrees of orientation and to exclude the influence of crystallization, amorphous PLLA rectangle samples (120-0 min) were stretched to different strains uniaxially at 60 °C with the stretching rate of 20 mm/min. Different positions were marked on the original bars. It is found in Fig. S2(a) that the strain of every marked length is consistent, which provides us proof for our assumption that the orientation of different positions on the tensile bar is similar. Taking 60-20-4 as an example, 2D WAXD patterns of different positions on the tensile bar are shown in Fig. S2(b) to verify the degree of orientation. It shows that WAXD diffractions of the three different positions are almost the same on the meridian and the isotropic scattering halo develops into the two arcs along the meridian. From the azimuth scan curve, it can be seen that the curves of the "upper, middle, down" parts are basically also the same. These results indicate that degrees of orientation of different positions along drawing direction of the tensile bar are the same, and the differences are negligible. This facilitates subsequent preparation of specimens for tests of in-plane thermal diffusivity.

The middle part of PLLA bars stretched to different strains is chosen to measure the degrees of orientation by 2D WAXD. The 2D WAXD patterns are shown in Fig. 5. The un-stretched PLLA shows regular concentric rings, indicating that the initial PLLA bar is amorphous and isotropic. With the increase in tensile strain, the isotropic halo gradually concentrates to the meridian, which indicates that amorphous chains of PLLA samples get orientated gradually along the drawing direction, and the strength increases gradually. In this process, no obvious crystal diffraction occurs. The meridian intensity profiles extracted from the WAXD patterns in Fig. 5b also show a very broad scattering peak of amorphous phase without any traces of crystalline phases. These results clearly demonstrated that the stretched PLLA bars with different strains are all amorphous and a series of PLLA with different degrees of orientation have been achieved to further reveal the influence of orientation on the thermal conductivity of PLLA.

Both the in-plane and through-plane thermal diffusivity of the stretched and un-stretched PLLA samples were measured at 25 °C. The thermal

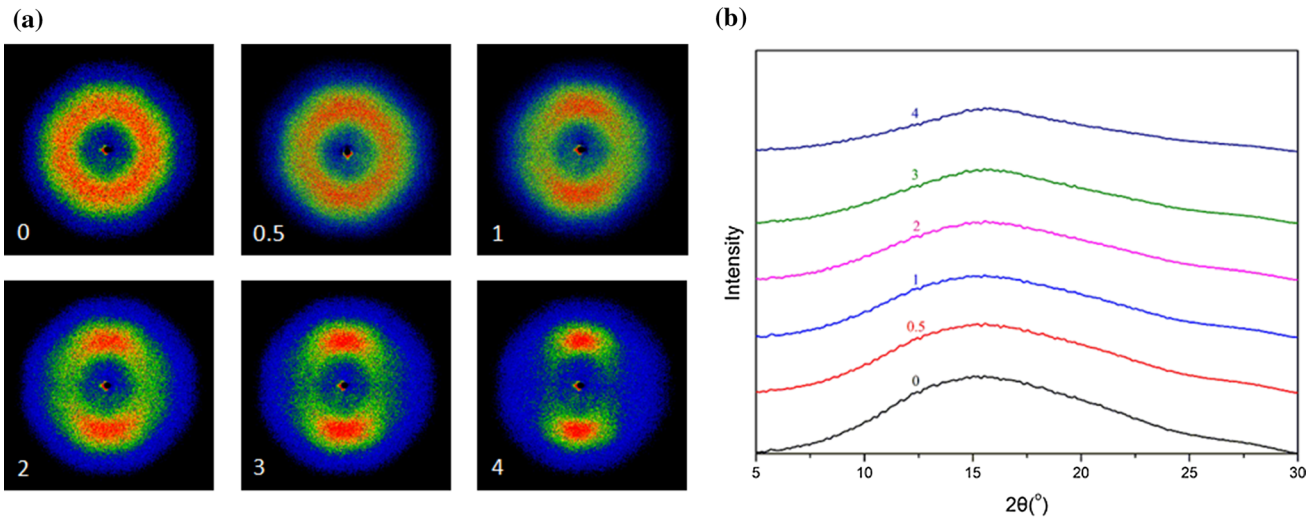

Figure 5 2D WAXD patterns (**a**) of PLLA samples stretched to different strains at 60 °C with the speed of 20 mm/min and meridian intensity profiles (**b**) extracted from the WAXD patterns.

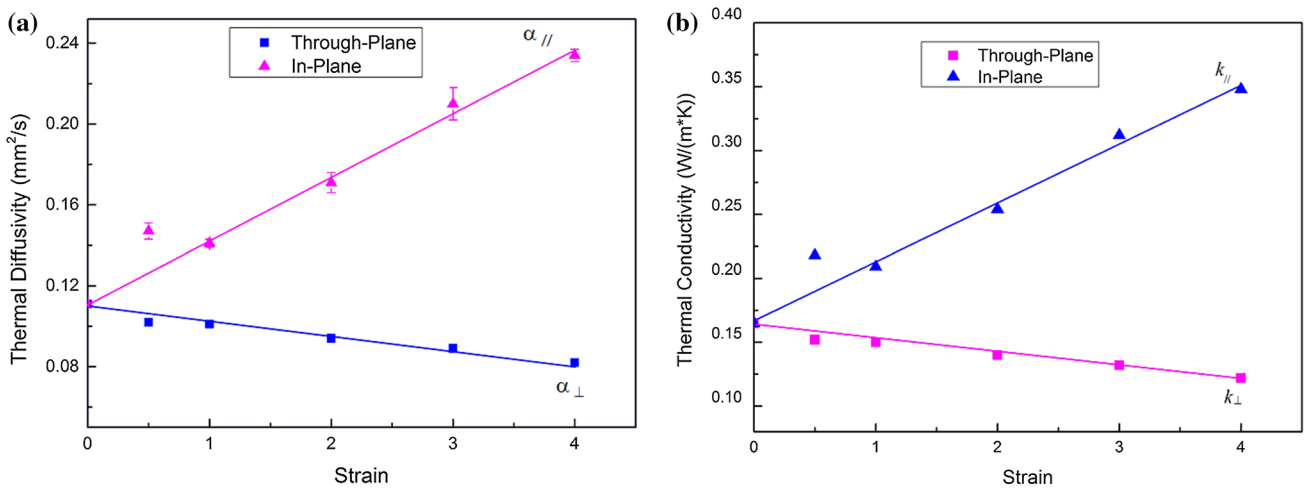

Figure 6 Thermal diffusivity (**a**) and conductivity of amorphous PLLA stretched samples (**b**) in through-plane and in-plane direction versus tensile strain.

conductivities are calculated by Eq. (2). Here, the specific heat and the density are constant, which are the values of the aforementioned PLLA 120-0 min (specific heat: 1.195 J/g K, density: 1.243 g/cm^3). The results are shown in Fig. 6. The relation between thermal diffusivity in the in-plane direction and tensile strain is opposite to the relation between thermal diffusivity in the through-plane direction and tensile strain. The thermal diffusivity in the in-plane direction increases as the tensile strain increases, while the thermal diffusivity of PLLA samples in the through-plane direction decreases with the increase in tensile strain. This is owing to that the thermal energy transports more efficiently parallel to the tensile direction, i.e., along the polymer chain, which consists of the strong covalent bonds, than perpendicular to the polymer chain, where the thermal energy is carried by the means of weak van der Waals interaction of molecules [22]. That is to say, the phonon mean free path along the tensile direction (in-plane direction) is larger than that perpendicular to the tensile direction (through-plane direction). Therefore, with the increase in orientation, the thermal diffusivity in the in-plane direction increases, while the one in the through-plane direction decreases. As the specific heat and density are constant, the variation of thermal conductivity (k) with the degree of orientation is consistent with the variation of the thermal diffusivity with the degree of orientation. The thermal conductivity in the in-plane direction ($k_{//}$) increases linearly with the increase in tensile strain, and thermal conductivity in the through-plane direction ($k_{\perp}$) decreases linearly with the increase in tensile strain. When the tensile strain is 4, the TC in the in-plane direction of PLLA is 0.348 W/mK, while the TC in the through-plane direction decreases to 0.125 W/mK. The relative thermal conductivities (k/k_0)-strain data are also given in Fig. 7, showing that the relative in-plane thermal conductivity ($k_{//}/k_0$) is low, only around 2 when tensile strain reaches to 4. Such a linear relationship between k ($k_{//}$ and $k_{\perp}$) and strain and low relative in-plane thermal conductivity have also been observed previously for other amorphous polymers such as PS, PMMA, PC, etc. [30, 32].

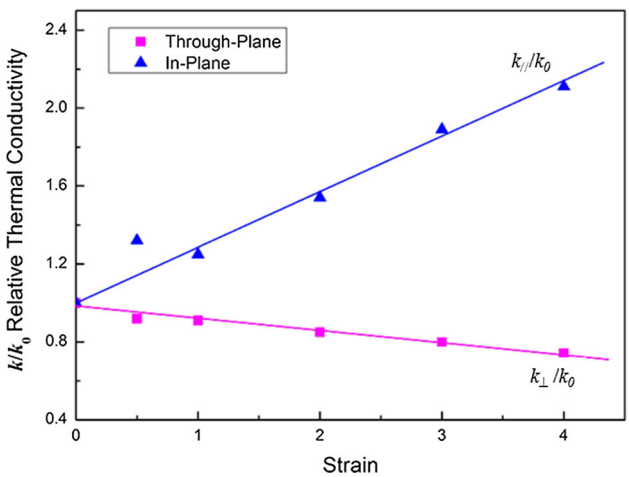

Figure 7 Relative thermal conductivity versus tensile strain for amorphous PLLA samples.

Table 3 Relationship between the conductivity of the oriented and unoriented PLLA samples

Sample code	60-20-0	60-20-0.5	60-20-1	60-20-2	60-20-3	60-20-4
$3/k_0$	18.2					
$(1/k_{//}) + (2/k_{\perp})$	18.2	17.8	18.1	18.3	18.3	19.3

A specific prediction of relationship between the conductivity of the oriented material and unoriented material has been given as Eq. (3).

$$3/k_0 = (1/k_{//}) + (2/k_{\perp}) \quad (3)$$

TC in the directions parallel and perpendicular to tensile direction would be principal conductivities which would indeed bear the relationship of Eq. (3) to a neutral plane conductivity in uniaxially oriented polymer. However, there is no fundamental reason why this neutral plane conductivity is the same as the conductivity of an unoriented specimen [32]. The corresponding parameters in Eq. 3 of PLLA are listed in Table 3. It is found that the thermal conductivities of the oriented and unoriented PLLA conform with the relationship of Eq. 3.

Conclusion

In this work, different crystallinity and degree of orientation of PLLA were fabricated by isothermal crystallization at 120 °C for different minutes and stretching the amorphous PLLA bars at 60 °C at the same speed to different strains, respectively. We have demonstrated the effect of temperature, crystallinity and degree of orientation on the thermal conductivity of bulk PLLA samples. The thermal conductivity of PLLA with different crystallinity was affected obviously by temperature. Before T_g, the thermal conductivity of PLLA with different crystallinity increases with temperature, mainly resulting from the increasing specific heat. As the temperature is further increased to be higher than T_g, the thermal conductivity of PLLA with different crystallinity decreases remarkably due to the obvious drop of thermal diffusivity. It demonstrates that thermal conductivity of PLLA increases with the increase in crystallinity, but the increasing rate is quite limited. With orientation, the conductivity was increased in the direction of molecular orientation and decreased in the perpendicular direction. The reciprocal of the two thermal conductivities in different directions of PLLA stretched to different strains fit a linear relationship.

Acknowledgements

This work was funded by the National Natural Science Foundation of China (51422305 and 51721091) and Sichuan Provincial Science Fund for Distinguished Young Scholars (2015JQO003).

Electronic supplementary material: The online version of this article (https://doi.org/10.1007/s10853-018-2306-4) contains supplementary material, which is available to authorized users.

References

[1] Olowojoba GB, Kopsidas S, Eslava S, Gutierrez ES, Kinloch AJ, Mattevi C, Rocha VG, Taylor AC (2017) A facile way to produce epoxy nanocomposites having excellent thermal conductivity with low contents of reduced graphene oxide. J Mater Sci 52:7323–7344. https://doi.org/10.1007/s10853-017-0969-x

[2] Wang Z, Cheng Y, Wang H, Yang M, Shao Y, Chen X, Tanaka T (2017) Sandwiched epoxy–alumina composites with synergistically enhanced thermal conductivity and breakdown strength. J Mater Sci 52:4299–4308. https://doi.org/10.1007/s10853-016-0511-6

[3] Yang J, Zhang E, Li XF, Zhang Y, Qu J, Yu Z-Z (2016) Cellulose/graphene aerogel supported phase change composites with high thermal conductivity and good shape stability for thermal energy storage. Carbon 98:50–57

[4] Yang J, Tang LS, Bao RY, Bai L, Liu ZY, Yang W, Xie BH, Yang MB (2016) Ice-templated assembly strategy to construct graphene oxide/boron nitride hybrid porous scaffolds in phase change materials with enhanced thermal conductivity and shape stability for light-thermal-electric energy conversion. J Mater Chem A 4:18841–18851

[5] Feng CP, Ni HY, Chen J, Yang W (2016) A facile method to fabricate highly conductive graphite/PP composite with

network structures. ACS Appl Mater Interfaces 8:19732–19738

[6] Yang J, Tang LS, Bao RY, Bai L, Liu ZY, Xie BH, Yang MB, Yang W (2018) Hybrid network structure of boron nitride and graphene oxide in shape-stabilized composite phase change materials with enhanced thermal conductivity and light-to-electric energy conversion capability. Sol Energy Mater Sol Cells 174C:56–64

[7] Feng CP, Bai L, Bao RY, Liu ZY, Yang MB, Chen J, Yang W (2018) Electrically insulating POE/BN elastomeric composites with high through-plane thermal conductivity fabricated by two-roll milling and hot compression. Adv Compos Hybrid Mater 1:160–167

[8] Chen H, Ginzburg VV, Yang J, Yang Y, Liu W, Huang Y, Du L, Chen B (2016) Thermal conductivity of polymer-based composites: fundamentals and applications. Prog Polym Sci 59:41–85

[9] Han Z, Fina A (2011) Thermal conductivity of carbon nanotubes and their polymer nanocomposites: a review. Prog Polym Sci 36:914–944

[10] Shen X, Wang Z, Wu Y, Liu X, He YB, Kim JK (2016) Multilayer graphene enables higher efficiency in improving thermal conductivities of graphene/epoxy composites. Nano Lett 16(6):3585–3593

[11] Noh YJ, Kim SY (2015) Synergistic improvement of thermal conductivity in polymer composites filled with pitch based carbon fiber and graphene nanoplatelets. Polym Test 45:132–138

[12] Zhao W, Kong J, Liu H, Zhuang Q, Gu J, Guo Z (2016) Ultra-high thermally conductive and rapid heat responsive poly(benzobisoxazole) nanocomposites with self-aligned graphene. Nanoscale 8:19984–19993

[13] Zhang WB, Zhan ZX, Yang JH et al (2015) Largely enhanced thermal conductivity of poly(vinylidene fluoride)/carbon nanotube composites achieved by adding graphene oxide. Carbon 90:242–254

[14] Yang J, Yu P, Tang LS, Bao RY, Liu ZY, Yang MB, Yang W (2017) Hierarchically well-ordered porous scaffolds for phase change materials with improved thermal conductivity and efficient solar-to-electric energy conversion. Nanoscale 9(45):17704–17709

[15] Yang J, Tang LS, Bao RY, Bai L, Liu ZY, Yang W, Xie BH, Yang MB (2017) Largely enhanced thermal conductivity of polyethylene glycol/boron nitride composite phase change materials for solar–thermal–electric energy conversion and storage with very low content of graphene nanoplatelets. Chem Eng J 315:481–490

[16] Xiao YJ, Wang WY, Lin T, Chen XJ, Zhang YT, Yang JH, Wang Y, Zhou ZW (2016) Largely enhanced thermal conductivity and high dielectric constant of poly(vinylidene fluoride)/boron nitride composites achieved by adding a few carbon nanotubes. J Phys Chem C 120:6344–6355

[17] Anderson DR (1966) Thermal conductivity of polymers. Chem Rev 1966:677–690

[18] Hansen D, Bernier GA (1972) Thermal-conductivity of polyethylene: effects of crystal size, density and orientation on thermal-conductivity. Polym Eng Sci 12:204–208

[19] Choy CL, Greig D (1975) Low-temperature thermal-conductivity of a semi-crystalline polymer, polyethylene terephthalate. J Phys C Solid State Phys 8:3121–3130

[20] Choy CL, Kwok KW, Leung WP, Lau FP (1994) Thermal-conductivity of poly(ether ether ketone) and its short-fiber composites. J Polym Sci Part B Polym Phys 32:1389–1397

[21] Yu J, Sundqvist B, Tonpheng B, Andersson O (2014) Thermal conductivity of highly crystallized polyethylene. Polymer 55:195–200

[22] Kurabayashi K (2001) Anisotropic thermal properties of solid polymers. Int J Thermophys 22:277–288

[23] Choy CL, Luk WH, Chen FC (1978) Thermal-conductivity of highly oriented polyethylene. Polymer 19:155–162

[24] Kanamoto T, Tsuruta A, Tanaka K, Takeda M, Porter RS (1988) Superdrawing of ultrahigh molecular-weight polyethylene 1 effect of techniques on drawing of single-crystal mats. Macromolecules 21:470–477

[25] Anandakumaran K, Roy SK, Manley RS (1988) Drawing-induced changes in the properties of polyethylene fibers prepared by gelation crystallization. Macromolecules 21:1746–1751

[26] Choy CL, Fei Y, Xi TG (1993) Thermal-conductivity of gel-spun polyethylene fibers. J Polym Sci Part B Polym Phys 31:365–370

[27] Mergenthaler DB, Pietralla M, Roy S, Kilian HG (1992) Thermal-conductivity in ultraoriented polyethylene. Macromolecules 25:3500–3502

[28] Saeidijavash M, Garg J, Grady B, Smith B, Li Z, Young RJ, Tarannum F, Bel Bekri N (2017) High thermal conductivity through simultaneously aligned polyethylene lamellae and graphene nanoplatelets. Nanoscale 9:12867–12873

[29] Choy CL, Chen FC, Luk WH (1980) Thermal-conductivity of oriented crystalline polymers. J Polym Sci Part B Polym Phys 18:1187–1207

[30] Hennig J (1967) Anisotropy and structure in uniaxially stretched amorphous high polymers. J Polym Sci Part C Polym Symp 16:2751–2761

[31] Choy CL (1977) Thermal-conductivity of polymers. Polymer 18:984–1004

[32] Washo BD, Hansen D (1969) Heat conduction in linear amorphous high polymers-orientation anisotropy. J Appl Phys 40:2423–2427

[33] Algaer EA, Alaghemandi M, Boehm MC, Mueller-Plathe F (2009) Anisotropy of the thermal conductivity of stretched amorphous polystyrene in supercritical carbon dioxide studied by reverse nonequilibrium molecular dynamics simulations. J Phys Chem B 113:14596–14603

[34] Singh V, Bougher TL, Weathers A, Cai Y, Bi K, Pettes MT, McMenamin SA, Lv W, Resler DP, Gattuso TR, Altman DH, Sandhage KH, Shi L, Henry A, Cola BA (2014) High thermal conductivity of chain-oriented amorphous polythiophene. Nat Nanotechnol 9:384–390

[35] Lu C, Chiang SW, Du H, Li J, Gan L, Zhang X, Chu X, Yao Y, Li B, Kang F (2017) Thermal conductivity of electrospinning chain-aligned polyethylene oxide (PEO). Polymer 115:52–59

[36] Takagi H, Kako S, Kusano K, Ousaka A (2007) Thermal conductivity of PLA-bamboo fiber composites. Adv Compos Mater 16:377–384

[37] Nakamura A, Iji M (2011) Factors affecting the magnitudes and anisotropies of the thermal and electrical conductivities of poly(L-lactic) acid composites with carbon fibers of various sizes. J Mater Sci 46:747–751. https://doi.org/10.1007/s10853-010-4807-7

[38] Tarawneh MA, Shahdan D, Ahmad SH (2013) Investigation on the effect of NiZn Ferrite on the mechanical and thermal conductivity of PLA/LNR nanocomposites. J Nanomater. https://doi.org/10.1155/2013/306961

[39] Huang J, Zhu Y, Xu L, Chen J, Jiang W, Nie X (2016) Massive enhancement in the thermal conductivity of polymer composites by trapping graphene at the interface of a polymer blend. Compos Sci Technol 129:160–165

[40] Mosanenzadeh SG, Khalid S, Cui Y, Naguib HE (2016) High thermally conductive PLA based composites with tailored hybrid network of hexagonal boron nitride and graphene nanoplatelets. Polym Compos 37:2196–2205

[41] Lebedev SM, Gefle OS, Amitov ET, Berchuk DY, Zhuravlev DV (2017) Poly(lactic acid)-based polymer composites with high electric and thermal conductivity and their characterization. Polym Test 58:241–248

[42] Luyt AS, Gasmi S (2016) Influence of blending and blend morphology on the thermal properties and crystallization behaviour of PLA and PCL in PLA/PCL blends. J Mater Sci 51:4670–4681. https://doi.org/10.1007/s10853-016-9784-z

[43] Li L, Cao ZQ, Bao RY, Xie BH, Yang MB, Yang W (2017) Poly(L-lactic acid)-polyethylene glycol-poly(L-lactic acid) triblock copolymer: a novel macromolecular plasticizer to enhance the crystallization of poly(L-lactic acid). Eur Polym J 97:272–281

[44] Meng XT, Bocharova V, Tekinalp H, Cheng SW, Kisliuk A, Sokolov AP, Kunc V, Peter WH, Ozcan S (2018) Toughening of nanocellulose/PLA composites via bio-epoxy interaction: mechanistic study. Mater Des 139(5):188–197

[45] Bao RY, Yang W, Jiang WR, Liu ZY, Xie BH, Yang MB (2013) Polymorphism of racemic poly(L-lactide)/poly(D-lactide) blend: effect of melt and cold crystallization. J Phys Chem B 117:3667–3674

[46] Renouf-Glauser AC, Rose J, Farrar DF, Cameron RE (2005) The effect of crystallinity on the deformation mechanism and bulk mechanical properties of PLLA. Biomaterials 26:5771–5782

[47] Zhang L, Zhang W, Cai G, Fu X (2012) Study on the thermal property parameters of PLA. China Plast Ind 40:68–71

[48] dos Santos WN, de Sousa JA, Gregorio R Jr (2013) Thermal conductivity behaviour of polymers around glass transition and crystalline melting temperatures. Polym Test 32:987–994

[49] Zarandi MB, Bioki HA, Mirbagheri ZA, Tabbakh F, Mirjalili G (2012) Effect of crystallinity and irradiation on thermal properties and specific heat capacity of LDPE & LDPE/EVA. Appl Radiat Isot 70:1–5